

Fluorescent Sensor for  $\text{Cu}^{2+}$  with a Tunable Emission WavelengthAndriy Mokhir,<sup>\*,†</sup> Alexander Kiel,<sup>‡</sup> Dirk-Peter Herten,<sup>‡</sup> and Roland Kraemer<sup>†</sup>*Institute of Inorganic Chemistry, Ruprecht-Karls-Universität Heidelberg, Im Neuenheimer Feld 270, 69120 Heidelberg, Germany, and Institute of Physical Chemistry, Ruprecht-Karls-Universität Heidelberg, Im Neuenheimer Feld 253, D-69120 Heidelberg, Germany*

Received March 9, 2005

A concept of fluorescent metal ion sensing with an easily tunable emission wavelength is presented and its principle demonstrated by detection of  $\text{Cu}^{2+}$ . A fluorescein dye was chemically modified with a metal chelating group and then attached to the terminus of ss-DNA. This was combined with a complementary ss-DNA modified with another fluorescent dye (ATTO 590), emitting at a longer wavelength. In the assembled duplex, fluorescence resonance energy transfer (FRET) between the fluorescein donor (excited at 470 nm) and the ATTO 590 acceptor (emitting at 624 nm) is observed. Proper positioning within the rigid DNA double helix prevents intramolecular contact quenching of the two dyes. Coordination of paramagnetic  $\text{Cu}^{2+}$  ions by the chelating unit of the sensor results in direct fluorescence quenching of the fluorescein dye and indirect (by loss of FRET) quenching of the ATTO 590 emission at 624 nm. As a result, emission of the acceptor dye can be used for monitoring of the concentration of  $\text{Cu}^{2+}$ , with a 20 nM detection limit. The emission wavelength is readily tuned by replacement of ATTO-DNA by other commercially available DNA-acceptor dye conjugates. Fluorescent metal ion sensors emitting at  $>600$  nm are very rare. The possibility of tuning the emission wavelength is important with respect to the optimization of this sensor type for application to biological samples, which usually show broad autofluorescence at  $<550$  nm.

## Introduction

Fluorescent molecular metal ion sensors become increasingly important as tools for the quantitative real-time monitoring of metal ion concentration in biological samples.<sup>1</sup> In such sensors, a metal chelating site is usually linked to fluorophore, and metal binding affects the fluorescence intensity of the compound. The majority of existing sensors are based on fluorophores such as fluorescein,<sup>2</sup> dansyl,<sup>3</sup> and

anthracene,<sup>1a,f,4</sup> which emit at wavelengths of  $<550$  nm. While such sensors are useful in various biological applications including live cell monitoring of more abundant metal ions ( $\text{Ca}^{2+}$ ,  $\text{Zn}^{2+}$ , and  $\text{Mg}^{2+}$ ), the broad emission at  $<550$  nm of biological samples (autofluorescence<sup>5</sup>) limits the sensitivity of analysis. Therefore, the development of sensors that emit above 600 nm, where autofluorescence is minimal, is desirable. Fluorescent metal ion sensors emitting at  $>600$  nm are very rare.<sup>6</sup>

A number of such red-emitting dyes are commercially available, but they are usually expensive, and the chemistry

\* To whom correspondence should be addressed. E-mail: Andriy.Mokhir@urz.uni-heidelberg.de. Tel: +49-6221-548441. Fax: +49-6221-548439.

<sup>†</sup> Institute of Inorganic Chemistry.

<sup>‡</sup> Institute of Physical Chemistry.

- (1) Selected reviews: (a) Jiang, P.; Guo, Z. *Coord. Chem. Rev.* **2004**, *248*, 205–229. (b) Pina, F.; Bernardo, M. A.; Garcia-Espana, E. *Eur. J. Inorg. Chem.* **2000**, 2143–2157. (c) Fabbrizzi, L.; Licchelli, M.; Pallavicini, P.; Parodi, L.; Taglietti, A. *Perspect. Supramol. Chem.* **1999**, *5*, 93–134. (d) Krämer, R. *Angew. Chem.* **1998**, *110*, 804–806. (e) de Silva, A. P.; Gunaratne, H. Q. N.; Gunnlaugsson, T.; Huxley, A. J. M.; McCoy, C. P.; Rademacher, J. T.; Rice, T. E. *Chem. Rev.* **1997**, *97*, 1515–1566. (f) Fabbrizzi, L.; Licchelli, M.; Pallavicini, P.; Perotti, A.; Taglietti, A.; Sacchi, D. *Chem. Eur. J.* **1996**, *2*, 75–82. Selected recent reports on fluorescent  $\text{Zn}^{2+}$  and  $\text{Cu}^{2+}$  sensors: (g) Meallet-Renault, R.; Pansu, R.; Amigoni-Gerbier, S.; Larpent, C. *Chem. Commun.* **2004**, 2344–2345. (h) Woodroffe, C. C.; Masalha, R.; Barnes, K. R.; Frederickson, C. J.; Lippard, S. J. *Chem. Biol.* **2004**, *11* (12), 1659–1666. (i) Chang, C. J.; Jaworski, J.; Nolan, E. M.; Sheng, M.; Lippard, S. J. *Proc. Natl. Acad. Sci. U.S.A.* **2004**, *101* (5), 1129–1134.

- (2) (a) Chavez-Crooker, P.; Garrido, N.; Ahearn, G. A. *J. Exp. Biol.* **2001**, *204*, 1433–1444. (b) Breuer, W.; Epsztejn, S.; Millgram, P.; Cabantchik, I. Z. *Am. J. Physiol.* **1995**, *268* (6, Part 1), C1354–1361. (3) (a) Corradini, R.; Dossena, A.; Galaverna, G.; Marchelli, R.; Panagia, A.; Sartor, G. *J. Org. Chem.* **1997**, *62*, 6283–6289. (b) Lin, W. Y.; Van Wart, H. E. *J. Inorg. Biochem.* **1998**, *32*, 21–38. (c) Zheng, Y.; Gattas-Asfura, K. M.; Konka, V.; Leblanc, R. M. *Chem. Commun.* **2002**, 2350–2351. (d) Torrado, A.; Walkup, G. K.; Imperiali, B. *J. Am. Chem. Soc.* **1998**, *120* (3), 609–610. (4) (a) Fabbrizzi, L.; Licchelli, M.; Pallavicini, P.; Perotti, A.; Sacchi, D. *Angew. Chem., Int. Ed. Engl.* **1994**, *106*, 2051–2053. (5) Billinton, N.; Knight, A. W. *Anal. Biochem.* **2001**, *291*, 175–197. (6) (a) Dujols, V.; Ford, F.; Czarnik, A. W. *J. Am. Chem. Soc.* **1997**, *119*, 7386–7387. (b) Gunnlaugsson, T.; Leonard, J. P.; Sénéchal, K.; Harte, A. J. *Chem. Commun.* **2004**, *7*, 782–783. (c) Klein, G.; Kaufmann, D.; Schürch, S.; Reymond, J.-L. *Chem. Commun.* **2001**, 561–562.

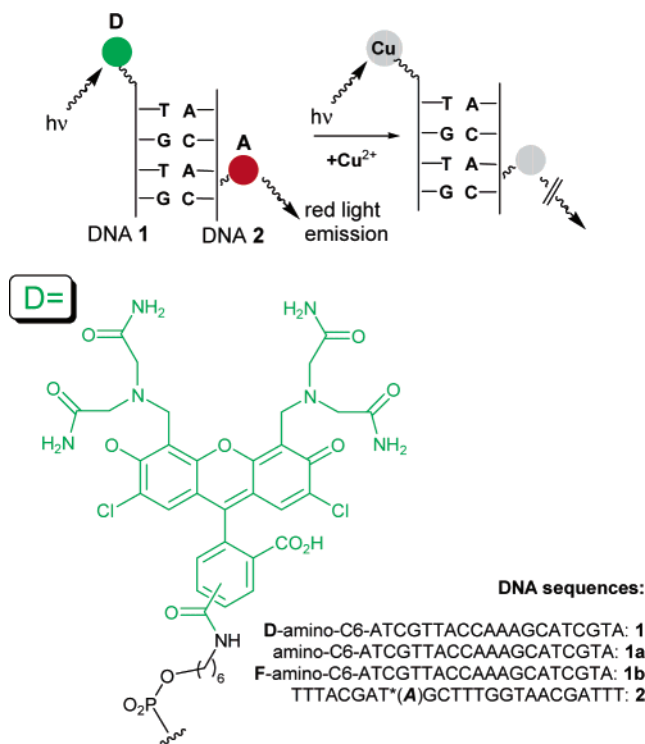


**Figure 1.** Concept of a fluorescent  $\text{Cu}^{2+}$  sensor with a tunable emission wavelength. Amino-C6 is a  $\text{H}_2\text{N}-(\text{CH}_2)_6-\text{OP}(\text{O})(\text{OH})-$  linker. The donor dye (D) is shown in green, and the acceptor dye (A) is in red. A is attached to a modified T-nucleobase, T\*. DNA 1 is a metal ion binding module, and DNA 2 is a sensing module.

of their directed functionalization for metal ion complexation is not well developed. We describe here a modular approach of sensor development, which relies on the assembly of complementary DNA strands and allows facile variation of the emitter dye wavelength by simply using commercially available fluorophore–DNA conjugates. The metal-binding module is a DNA conjugate of chelator-modified fluorescein. The signaling module is a red-emitting dye attached to a complementary DNA strand. In the duplex between these DNA conjugates, efficient fluorescence resonance energy transfer (FRET<sup>7</sup>) will take place upon excitation of the fluorescein chromophore and result in red light emission of the signaling chromophore. At the same time, the rigid structure of the DNA double helix will prevent contact quenching of fluorescein and the red-emitting dye (Figure 1). This complication would lead to a loss of sensor fluorescence with (instead of ds-DNA) a simple covalent linker, which allows close proximity of the two chromophores.

The strength of our approach is in its versatility. Variation of the chelating unit at the metal-binding fluorescein module allows tuning of the binding affinity and metal ion selectivity; a number of chelating fluorescein derivatives have been described.<sup>1h,i,2,8</sup> The second module, DNA conjugates of red-emitting dyes such as Cy3, Cy5, TMR, and ATTO series, is commercially available. Consequently, tuning of the emission wavelength for optimal application-dependent requirements is straightforward.

We demonstrate the described principle by detection of  $\text{Cu}^{2+}$  ions.  $\text{Cu}^{2+}$  is a less abundant but important trace metal ion in biological samples. For example, in blood serum, copper is bound in the 2+ state by ceruloplasmin and albumin,<sup>9</sup> and detection of serum copper levels is relevant to monitoring of various disease states. In Alzheimer's disease,  $\text{Cu}^{2+}$  is enriched in brain tissues containing  $\beta$ -amyloid plaques.<sup>10</sup> Although in the cytoplasm Cu is mostly present in the 1+ state and tightly bound to proteins, some intracellular enzymes in their resting state contain  $\text{Cu}^{2+}$ .<sup>11</sup>

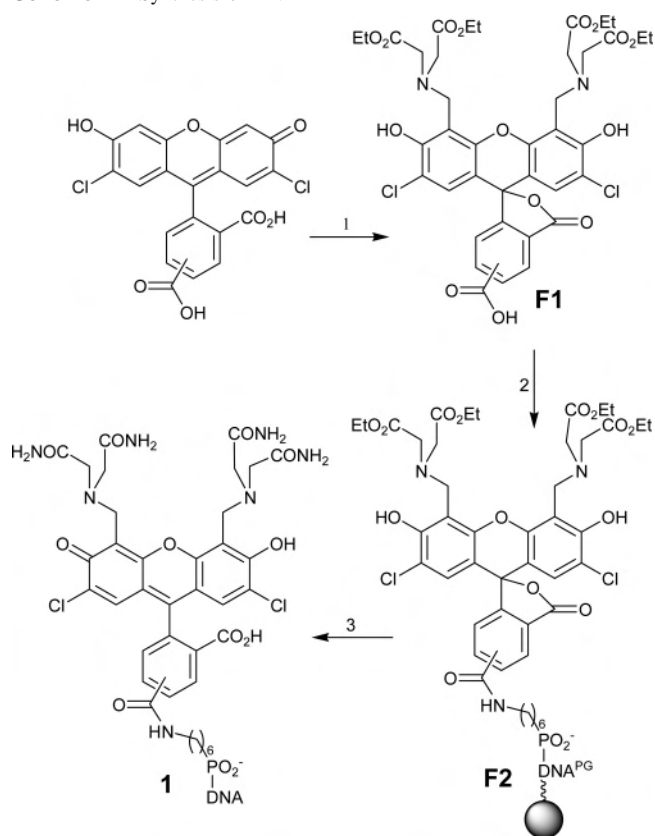
## Experimental Section

The best commercially available chemicals from Aldrich/Sigma/Fluka (Deisenhofen, Germany) were obtained and used without purification. The reagents for DNA synthesis were obtained from Prologo (Hamburg, Germany) and Glen Research (Eurogentec, Belgium). Unmodified HPLC-purified DNAs were obtained from Metabion (Martinsried, Germany). MALDI-TOF mass spectra were recorded on a Bruker BIFLEX III spectrometer. The mixture of a  $\text{CH}_3\text{CN}$ -saturated solution of azathiothymine (ATT) and a 0.1 M aqueous diammonium citrate solution (2:1) was used as a matrix for MALDI-TOF analysis of DNA conjugates. Samples for mass spectrometry were prepared on a Bruker MAP II probe preparation station using a dried droplet method with a 1:2 probe/matrix ratio. The mass accuracy with external calibration was 0.1% of the peak mass, i.e.,  $\pm 6.0$ , at  $m/z$  6000. Preparative and analytical HPLC was performed at 22 °C on a Shimadzu liquid chromatograph equipped with a UV–vis detector, a column oven, and an Advantec SF-2100W fraction collector. A Macherey-Nagel Nucleosil C4 250  $\times$  4.6 mm column with gradients of  $\text{CH}_3\text{CN}$  (solvent B) in water (50 mM triethylammonium acetate, pH 7, solvent A) was used. <sup>1</sup>H NMR spectra were recorded on a 400 MHz Varian NMR spectrometer. A Varian Cary 100 Bio UV–vis spectrophotometer was used for UV–melting experiments and measurements of UV–visible spectra. Black wall semimicrocuvettes (1 cm) with a sample volume of 0.7 mL, which contained DNA strands (0.2  $\mu\text{M}$  of each) in a MOPS buffer (10 mM, pH 7) and NaCl (50 mM) with or without metal ions  $\text{M}^{2+}$  (0.6  $\mu\text{M}$ ), were used. Cooling and heating rates in UV–melting experiments were 0.5 °C/min. Melting points were averages of the extrema of the first derivative of the 61-point smoothed curves from at least two cooling and two heating curves. Fluorescent spectra were acquired on a Varian Cary Eclipse fluorescence spectrometer.

**Synthesis. F1 (Scheme 1, Step 1).** Paraformaldehyde (0.48 g, 16 mmol) and diethyliminodiacetate (1.51 g, 8 mmol) were added

- (8) (a) Chang, C. J.; Nolan, E. M.; Jaworski, J.; Okamoto, K.; Hayashi, Y.; Sheng, M.; Lippard, S. J. *Inorg. Chem.* **2004**, *43* (21), 6774–6779. (b) Nolan, E. M.; Burdette, S. C.; Harvey, J. H.; Hilderbrand, S. A.; Lippard, S. J. *Inorg. Chem.* **2004**, *43* (8), 2624–2635. (c) Burdette, S. C.; Frederickson, C. J.; Bu, W.; Lippard, S. J. *J. Am. Chem. Soc.* **2003**, *125* (7), 1778–1787. (d) Woodrooffe, C. C.; Lippard, S. J. *J. Am. Chem. Soc.* **2003**, *125* (38), 11458–11459. (e) Clark, M. A.; Duffy, K.; Tibrewala, J.; Lippard, S. J. *Org. Lett.* **2003**, *5* (12), 2051–2054.
- (9) (a) Linder, M. C.; Wooten, L.; Cerveza, P.; Cotton, S.; Shulze, R.; Lomeli, N. *Am. J. Clin. Nutr.* **1998**, *67* (5), 965S–971S. (b) Harford, C.; Sarkar, B. *Metal–Albumin Interactions*. In *Handbook of Metal–Ligand Interactions in Biological Fluids: Bioinorganic Chemistry*; Berthon, G., Ed.; Dekker: New York, 1995; Vol. 1, pp 405–410. (c) Sarkar, B. *Biol. Trace Elem. Res.* **1989**, *21*, 137–144.
- (10) (a) Karr, J. W.; Kaupp, L. J.; Szalai, V. A. *J. Am. Chem. Soc.* **2004**, *126* (41), 13534–13538. (b) Brown, D. R.; Kozlowski, H. *J. Chem. Soc., Dalton Trans.* **2004**, *13*, 1907–1917.
- (11) Masserschmidt, A.; Huber, R.; Poulos, T.; Wieghardt, K. *Handbook of metalloproteins*; John Wiley & Sons Ltd.: Chichester, England, 2001.

(7) (a) Förster, Th. *Ann. Phys.* **2**, 55–75. (b) Kikuchi, K.; Takakusa, H.; Nagano, T. *Trends Biotechnol.* **2004**, *22* (7), 363–370.

Scheme 1. Synthesis of DNA **1**<sup>a</sup>

<sup>a</sup> 1: HN(CH<sub>2</sub>CO<sub>2</sub>Et)<sub>2</sub>, CH<sub>2</sub>O. 2: DIEA, C6-amino-DNA-CPG. 3: aqueous NH<sub>3</sub>, 25%.

to acetonitrile (50 mL), and the suspension obtained was heated to reflux for 90 min. 2',7'-Dichlorofluorescein-5(6)-carboxylate (0.71 g, 1.6 mmol) in acetonitrile/water (1:1, 50 mL) was added, and the resulting solution was left stirring for 24 h. After cooling, CH<sub>3</sub>CN was removed by evaporation and the aqueous solution was acidified with acetic acid to pH 4, cooled to 4 °C, and left at this temperature for 2 h. The precipitate formed was filtered, washed with cold water, and dried at 0.01 mbar. The product was purified by silica gel chromatography using a CHCl<sub>3</sub>/EtOH (9:1) mixture containing 0.1% AcOH. The resulting bright orange solid is a mixture of two isomers in a ~4:1 molar ratio (6:5 isomers). Yield: 0.62 g, 42%. *R<sub>f</sub>*: 0.6 in a CHCl<sub>3</sub>/EtOH (1:5) mixture containing 0.1% AcOH. <sup>1</sup>H NMR (δ, ppm, relative to TMS): 9.59 (br s), 8.75 (s, 0.3H), 8.42 (dd, 0.3H, <sup>3</sup>J = 8.2 Hz, <sup>4</sup>J = 1.4 Hz), 8.37 (dd, 1H, <sup>3</sup>J = 8.0 Hz, <sup>4</sup>J = 1.2 Hz), 7.90 (s, 1H), 8.13 (dd, 1H, <sup>3</sup>J = 8.0 Hz, <sup>5</sup>J = 0.6 Hz), 7.3 (dd, 0.3H, <sup>3</sup>J = 8.0 Hz, <sup>5</sup>J = 0.8 Hz), 6.62 (s, 0.6H), 6.60 (s, 2H), 4.42 (d, 2H, <sup>2</sup>J = 14.3 Hz), 4.44 (d, 0.6H, <sup>2</sup>J = 14.3), 4.28 (m, 2.6H), 4.20 and 4.21 (two q, 10.4H, <sup>3</sup>J = 7.2 Hz), 3.60, 3.61 (two s, 10.4H), 2.11 (s, 3.9H), 1.27 (t, 15.6H, <sup>3</sup>J = 7.2 Hz). HR-ESI-MS, positive mode: calcd for C<sub>39</sub>H<sub>41</sub>Cl<sub>2</sub>N<sub>2</sub>O<sub>15</sub> ([M + H]<sup>+</sup>), 847.1883; found, 847.1862. CHN anal. Calcd for C<sub>41</sub>H<sub>48</sub>Cl<sub>2</sub>N<sub>2</sub>O<sub>19</sub> ((**F1**·CH<sub>3</sub>CO<sub>2</sub>H·(H<sub>2</sub>O)<sub>2</sub>): C, 52.2; H, 5.1; N, 3.0. Found: C, 52.03; H, 4.91; N, 3.36.

**DNA 1 (Scheme 1, Steps 2 and 3).** A mixture of **F1** (80 mg, 86 μmol), *N*-hydroxysuccinimide (12 mg, 100 μmol), and 1-ethyl-3-[3-(dimethylamino)propyl]carbodiimide hydrochloride (EDAC·HCl; 19 mg, 100 μmol) was dried at 0.01 mbar for 24 h, dissolved in DMF (1 mL), and allowed to react at 22 °C for 8 h. Water (9 mL) was added, and the product was extracted with ethyl acetate (3 × 10 mL). Combined organic extracts were dried over Na<sub>2</sub>SO<sub>4</sub> and solvent, all volatiles were removed, and the remaining oil was

dissolved in CHCl<sub>3</sub>. The solution was filtered through silica gel, and the solvent was removed to obtain **F2** (74 mg, bright orange solid, yield 91%). HR-ESI-MS: calcd for C<sub>43</sub>H<sub>44</sub>Cl<sub>2</sub>N<sub>3</sub>O<sub>17</sub> ([M + H]<sup>+</sup>), 944.2047; found, 944.2031. **F2** (47 mg, 50 μmol) was dissolved in DMF (200 μL), and diisopropylethylamine (DIEA; 19 mg, 150 μmol) was added. The solution obtained was added to controlled pore glass (CPG)-bound protected DNA, which contained a terminal-free amino group (C6-amino-DNA-CPG; 0.4 μmol of free amino groups). The mixture was agitated for 12 h using an automatic shaker. Then the solution was filtered, the CPG was washed with DMF (3 × 2 mL) and CH<sub>3</sub>CN (3 × 2 mL) and dried at 0.01 mbar, and the DNA conjugate was cleaved from the polymer and deprotected using aqueous ammonia (25%) at 22 °C for 24 h. The solution was filtered, the CPG was washed with water (300 μL), and the obtained aqueous solutions were combined, diluted with 9 volumes of water, and lyophilized. The product was dissolved in water and purified by HPLC: 0% B for 1.5 min, within 20 min to 30% B, within 6 min to 90% B, 90% B for 10 min. *R<sub>t</sub>*: 22 min. Yield: 17 nmol, 4.3%. MALDI-TOF MS: calcd for C<sub>232</sub>H<sub>285</sub>N<sub>79</sub>O<sub>129</sub>P<sub>20</sub>Cl<sub>2</sub> ([M - H]<sup>-</sup>), 6931.2; found, 6937.5.

**FRET Measurement.** For the determination of the Förster distance *R*<sub>0</sub> between **D1** and ATTO 590, eq 1 has been used (*R*<sub>0</sub> = 5.63 nm). The overlap integral *J*(λ) has been determined from emission and absorption spectra of **D1** and ATTO 590, respectively. We assumed free rotation of the dyes (*κ*<sup>2</sup> = 2/3). The relative quantum efficiency of **D1** has been determined to be *Q*<sub>D</sub> = 0.7 ± 2.

$$R_0^6 = \left( \frac{9000(\ln 10)Q_D\kappa^2}{128\pi^5 N n} \right) J(\lambda) \quad (1)$$

$$E = \frac{R_0^6}{R_0^6 + r^6} \quad (2)$$

Equation 2 gives the prediction for the FRET efficiency versus distance. For the measurement of FRET efficiencies, the emission of DNA **1** has been compared with the emission of the duplex DNA **1**/DNA **2**. The FRET efficiency has been determined to be 19 ± 5%, which corresponds to 74 + 4 Å between the dyes. Provided that the duplex DNA **1**/DNA **2** has a B-form structure and linkers between the dyes and DNA adopt extended conformations, the distance between the dyes is expected to be ~75 Å, which is in agreement with the experimental value.

## Results and Discussion

**Synthesis and Metal-Binding Properties of DNA 1.** Fluorescein derivative **F1** was synthesized from 2',7'-dichlorofluorescein-5(6)-carboxylate and diethyliminodiacetate in a Mannich reaction in accordance with the modified method reported for synthesis of analogous compounds.<sup>8d</sup> The 5(6)-carboxylic acid group of **F1** was activated using a mixture of carbodiimide reagent (EDAC) and *N*-hydroxysuccinimide and then reacted with the amino group of bound to solid-phase 5'-amino-modified DNA, which was fully protected except the terminal amino group. Finally, DNA **1** was obtained after its cleavage from the solid phase and deprotection of nucleobases and DNA backbone functional groups in concentrated aqueous ammonia and HPLC purification.

The Cu<sup>2+</sup> binding fragment in DNA **1** is a structural analogue of Calcein. The latter is a sensitive but unspecific

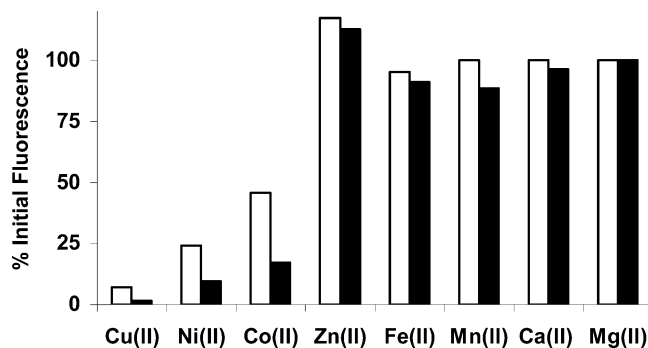


**Figure 2.** Effect of different metal ions on the fluorescence of DNA 1: DNA 1 (1  $\mu\text{M}$ ),  $\text{M}^{2+}$  (1  $\mu\text{M}$  white bars; 10  $\mu\text{M}$  black bars), MOPS (10 mM, pH 7), NaCl (50 mM), excitation at 514 nm, emission at 534 nm.

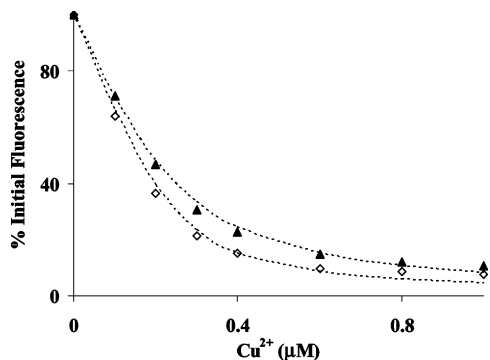


**Figure 3.** Titration of DNA 1 (filled diamonds) and the DNA 1/DNA 2 duplex (open squares) with  $\text{Cu}^{2+}$ : each strand (0.2  $\mu\text{M}$ ), MOPS (10 mM, pH 7), NaCl (50 mM), excitation at 514 nm, emission at 534 nm. Dotted lines represent theoretical titration curves calculated based on the model containing the unbound dye **D**,  $\text{Cu}^{2+}$ , and a 1:1  $\text{Cu}^{2+}$ /**D** complex.  $K = [\text{Cu}-\text{D}]/([\text{Cu}^{2+}][\text{D}])$ ;  $\log K(\text{Cu}/\text{DNA 1}) = 7.4$ , and  $\log K[\text{Cu}/(\text{DNA 1}/\text{DNA 2})] = 7.2$ .

fluorescent sensor for transition-metal ions.<sup>2b</sup> We have introduced a carboxylic group at the 5(6) position of Calcein for its conjugation with DNA and replaced carboxylic acid groups of iminodiacetate fragments with amide groups to improve selectivity of  $\text{Cu}^{2+}$  detection (dye **D**, Figure 1). Although Calcein itself discriminates poorly between  $\text{Cu}^{2+}$ ,  $\text{Ni}^{2+}$ , and  $\text{Co}^{2+}$  ions, fluorescence of DNA 1 is quenched by  $\text{Cu}^{2+}$  measurably better than by  $\text{Ni}^{2+}$  and  $\text{Co}^{2+}$  (Figure 2). Improved discrimination between  $\text{Cu}^{2+}$  and  $\text{Ni}^{2+}$  can be achieved because of their different kinetics of interaction with the sensor. In particular,  $\text{Cu}^{2+}$  binding (1 equiv) to DNA 1 (1  $\mu\text{M}$ ) is practically instantaneous, while  $\text{Ni}^{2+}$  binding at similar conditions is completed only  $\sim 5$  min after mixing the reagents. Other metal ions practically do not affect the fluorescence emission of DNA 1 (Figure 2). Analogous to parent Calcein, dye **D** has two sites for binding of metal ions. Therefore, DNA 1 may potentially form binuclear complexes along with mononuclear ones. Titrations of DNA 1 by  $\text{Cu}^{2+}$  (up to 5 equiv) monitored by changes in the fluorescence emission of dye **D** can be well fitted using a model containing free ligand,  $\text{Cu}^{2+}$  ions, and their 1:1 complex (Figure 3). This indicates that only one copper ion binds to DNA 1 at our experimental conditions. The stability of this 1:1 complex is rather high,  $\log K = 7.4 \pm 0.2$ . Complexes of  $\text{Cu}^{2+}$  with 5'-fluorescein-modified DNA have at least 2 orders of magnitude lower stabilities,  $\log K < 5$ ,<sup>12</sup> which indicates that in the 1:1 complex  $\text{Cu}^{2+}$  is bound to

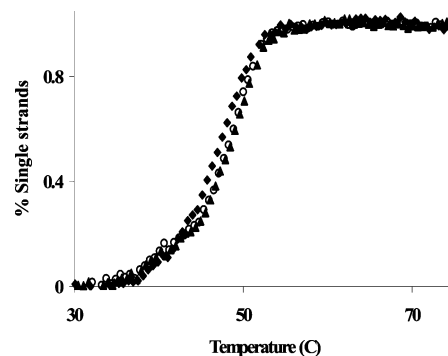


**Figure 4.** Melting profiles of DNA 1/DNA 2 (filled diamonds), DNA 1a/DNA 2 (filled triangles), and DNA 1b/DNA 2 (open circles) duplexes: each strand (0.2  $\mu\text{M}$ ), MOPS (10 mM, pH 7), NaCl (50 mM).

**Table 1.** Melting Temperatures of 1/2, 1a/2, and 1b/2 Duplexes in the Presence of  $\text{Cu}^{2+}$ ,  $\text{Ni}^{2+}$ , and  $\text{Zn}^{2+}$ <sup>a</sup>

DNA duplex	$T_m$ ( $^{\circ}\text{C}$ )			
	no metal ion	+ $\text{Cu}^{2+}$	+ $\text{Ni}^{2+}$	+ $\text{Zn}^{2+}$
1/2	$47.9 \pm 0.6$	$47.4 \pm 1.0$	$47.7 \pm 1.3$	$47.8 \pm 0.4$
1a/2	$49.5 \pm 0.1$	$49.7 \pm 0.5$	$49.7 \pm 1.3$	$49.5 \pm 0.3$
1b/2	$49.2 \pm 0.1$	$49.2 \pm 0.3$	$49.5 \pm 1.5$	$49.3 \pm 0.4$

<sup>a</sup> Each strand (0.2  $\mu\text{M}$ ), MOPS (10 mM, pH 7), NaCl (50 mM),  $\text{M}^{2+}$  (0.6  $\mu\text{M}$ ).

the chelating groups of dye **D** rather than to nucleobases or backbone donor groups of DNA 1. A peak corresponding to a 1:1  $\text{Cu}^{2+}$ /DNA 1 complex is observed in the MALDI-TOF mass spectrum of the probe prepared from solutions of DNA 1 and  $\text{CuSO}_4$  (both 0.18 mM) adjusted to pH 7 by  $\text{NEt}_3$ . At these conditions (higher concentration of the components), a peak corresponding to a 1:2 complex is also present. Mass spectra of DNA 1/ $\text{Cu}^{2+}$  mixtures at conditions used in fluorescence experiments could not be obtained. In the presence of excess  $\text{Cu}^{2+}$ , fluorescence of DNA 1 is practically fully quenched, which indicates that a 1:1  $\text{Cu}^{2+}$ /**D** complex is not fluorescent (Figure 3).

**Assembly of Metal-Binding Module DNA 1 and Signaling Module DNA 2.** Some chemical modifications decrease the binding affinity of DNA conjugates to their complementary strands.<sup>13</sup> Fortunately, the residue **D** only slightly destabilizes the duplex structure (Figure 4). In the presence of  $\text{Cu}^{2+}$ ,  $\text{Zn}^{2+}$ , and  $\text{Ni}^{2+}$  (3 equiv), melting points of the mentioned duplexes remain unchanged (Table 1). These experiments indicate that at 22  $^{\circ}\text{C}$  the duplex form is the only species in mixtures of DNA 1 and DNA 2 in both the presence and absence of the metal ions. It should be noted that in the presence of excess mentioned metal ions (3 equiv) no products of DNA decomposition could be detected by HPLC analysis even after 48 h at 22  $^{\circ}\text{C}$ . This indicates that at these conditions metal-promoted oxidative DNA cleavage is not relevant.  $\text{Cu}^{2+}$ -promoted cleavage of DNA has been reported but usually requires specific ligands and reducing

(12) Brunner, J.; Kraemer, R. *J. Am. Chem. Soc.* **2004**, *126* (42), 13626–13627.

(13) (a) Mokhir, A.; Tetzlaff, C. N.; Herzberger, S.; Mosbacher, A.; Richert, C. *J. Comb. Chem.* **2001**, *3* (4), 374–386. (b) Kryatova, O. P.; Connors, W. H.; Blecinski, C. F.; Mokhir, A.; Richert, C. *Org. Lett.* **2001**, *3* (7), 987–990.

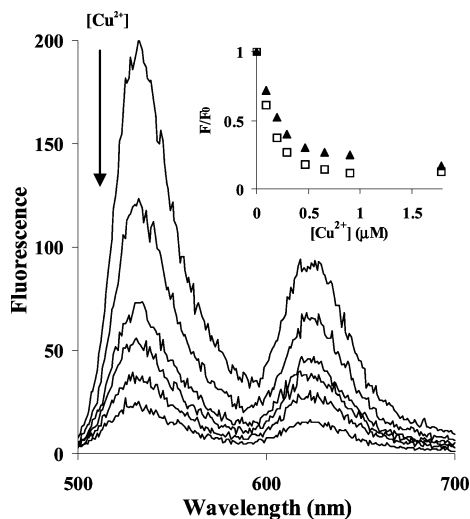


**Figure 5.** Fluorescence spectra (excitation at 470 nm) of a DNA 1/DNA 2 duplex (0.2  $\mu\text{M}$ ), MOPS (pH 7, 10 mM), and NaCl (50 mM) solution in the presence of different  $\text{Cu}^{2+}$  concentrations. Inset: dependence of  $F/F_0$  at 534 nm (open squares) and 624 nm (filled triangles) on the  $\text{Cu}^{2+}$  concentration.

agents (ascorbate and thiolates) or  $\text{H}_2\text{O}_2$  in large excess.<sup>14</sup> The kinetics of DNA 1/DNA 2 duplex formation has been studied by fluorescence spectroscopy using FRET between dye **D** of DNA 1 and ATTO 590 of DNA 2. The FRET efficiency is increased upon association of DNA strands. At 22 °C, the duplex is fully formed 20 min after mixing DNA 1 with DNA 2. This preequilibration time has been used in all further experiments. Association of DNA 1 with its complementary DNA 2 does not affect the kinetics of dye **D**/ $\text{Cu}^{2+}$  complex formation and only slightly decreases the stability of the latter ( $\log K = 7.2 \pm 0.1$ ). Along with the fact that the stability of the duplex DNA 1/DNA 2 is practically independent from the concentration of  $\text{M}^{2+}$ , these experiments suggest the absence of strong interactions between the dye **D** and DNA strands in the duplex.

**Detection of  $\text{Cu}^{2+}$  by the DNA 1/DNA 2 Sensor.** Absorption bands of DNA 1 and DNA 2 in the visible spectral region (chromophores of dye **D** and ATTO 590<sup>15</sup> correspondingly) are rather broad and partly overlap with each other. Selective excitation of dye **D** of DNA 1 in the presence of DNA 2 can be achieved using  $\leq 470$ -nm excitation wavelengths. For example, extinction at 470 nm ( $\epsilon_{470}$ ) of dye **D** (DNA 1) is still 39% of the extinction at its absorption maximum (514 nm), whereas  $\epsilon_{470}$  of ATTO 590 (DNA 2) is less than 2% of the extinction at its absorption maximum (594 nm). Therefore, direct excitation of ATTO 590 at 470-nm wavelength is negligible in the duplex DNA 1a/DNA 2 lacking dye **D**. In contrast, excitation of ATTO 590 at 470-nm wavelength in the duplex DNA 1/DNA 2 occurs because of FRET from dye **D** (Figure 5). In the presence of  $\text{Cu}^{2+}$  ions, the stable nonfluorescent 1:1  $\text{Cu}^{2+}$ /dye **D** complex is formed in a solution of DNA 1/DNA 2. Because of the loss of a suitable FRET donor, fluorescence

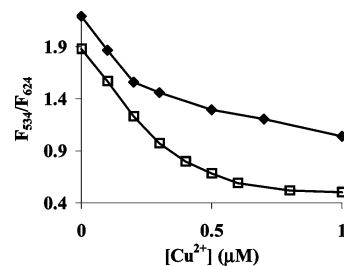


**Figure 6.** Dependence of the ratio of fluorescence intensities at 534 and 624 nm wavelengths ( $F_{534}/F_{624}$ ) of a DNA 1/DNA 2 duplex on the  $\text{Cu}^{2+}$  concentration: (filled squares) excitation at 470 nm; (open squares) excitation at 514 nm; duplex (0.2  $\mu\text{M}$ ), MOPS (10 mM, pH 7), NaCl (50 mM).

of ATTO 590 is also quenched by  $\text{Cu}^{2+}$  in an indirect manner. Consequently, the ATTO 590 quenching efficiency correlates with the amount of copper ions bound to DNA 1/DNA 2 and therefore can be used for monitoring the  $\text{Cu}^{2+}$  concentration (Figure 5). The DNA duplex loses its  $\text{Cu}^{2+}$ -sensing properties when dye **D** is substituted for a fluorescein derivative, which does not contain a strong  $\text{Cu}^{2+}$  binding motif. In particular, fluorescence of the corresponding duplex DNA 1b/DNA 2 is practically not dependent on the  $\text{Cu}^{2+}$  concentration (at  $\leq 10$  equiv of  $\text{Cu}^{2+}$ ). The lowest  $\text{Cu}^{2+}$  concentration detectable by DNA 1/DNA 2 (0.2  $\mu\text{M}$ ) was found to be 20 nM. A similar detection limit can be achieved by the usual fluorescence sensors for  $\text{Cu}^{2+}$  emitting at  $< 550$  nm (Fura-2,<sup>16</sup> Phen Green<sup>2a</sup>, and Calcein<sup>2b</sup>).  $\text{Cu}^{2+}$  affinity and sensitivity of our sensor can be improved by substitution of dye **D** of DNA 1 for a stronger  $\text{Cu}^{2+}$  binder. Fluorescein derivatives containing potentially efficient  $\text{Cu}^{2+}$  binding ligands have been reported.<sup>8</sup>

The emission wavelength of the acceptor ATTO 590 in the DNA 1/DNA 2 duplex is easily tuned by its replacement with other dyes. For example, conjugates of DNA with tetramethylrhodamine (TMR; emission at 580 nm) and 6-carboxy-4',5'-dichloro-2',7'-dimethoxyfluorescein (JOE; emission at 550 nm) have been tested. Analogous quenching effects of  $\text{Cu}^{2+}$  could be reproduced in these systems at optimal conditions.

Nucleases present in biological samples can potentially cleave the DNA-based sensor, producing dissociated fragments containing the donor and acceptor dyes. However, because biological buffers contain mostly single-strand specific nucleases, cleavage of sensors based on stable double-stranded DNAs is not expected to be a serious problem. We and others have confirmed that DNA duplexes are several times more stable than single-stranded DNA in the presence of typical 3'- and 5'-exonucleases and -endonucleases at physiological conditions.<sup>13a,17</sup>

**DNA 1/DNA 2 Duplex as a Ratiometric  $\text{Cu}^{2+}$  Sensor.** The ratio of fluorescent intensities of two emission bands of the DNA 1/DNA 2 duplex (Figure 5),  $F_{534}/F_{624}$ , is only slightly dependent on the  $\text{Cu}^{2+}$  concentration upon excitation at 470-nm wavelength. In particular, in the presence of excess

(14) Selected reviews on oxidative DNA cleavage: (a) Burrows, C. J.; Muller, J. G. *Chem. Rev.* **1998**, 98 (3), 1109–1151. (b) Pogozelski, W. K.; Tullius, T. D. *Chem. Rev.* **1998**, 98 (3), 1089–1108.  
(15) <http://www.atto-tec.de/>.

(16) McCall, K. A.; Fierke, C. A. *Anal. Biochem.* **2000**, 284, 307–315.  
(17) (a) Sarracino, D.; Richert, C. *Bioorg. Med. Chem. Lett.* **1996**, 6, 2543–2548. (b) Mokhir, A.; Richert, C. *Nucleic Acids Res.* **2000**, 28 (21), 4254–4265.

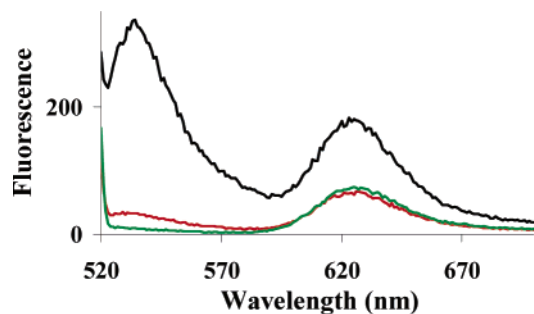


**Figure 7.** Fluorescence spectra (excitation at 514 nm) of DNA **2** (green line), a DNA **1**/DNA **2** duplex (black line), and DNA **1**/DNA **2** with 3 equiv of  $\text{Cu}^{2+}$  (red line): DNA (0.2  $\mu\text{M}$ ), MOPS (10 mM, pH 7), NaCl (50 mM).

$\text{Cu}^{2+}$  (5 equiv),  $F_{534}/F_{624} = 1.0$ , and in the absence of  $\text{Cu}^{2+}$ ,  $F_{534}/F_{624} = 2.2$  (Figure 6). Upon excitation of the duplex DNA **1**/DNA **2** at 514 nm (absorption maximum of **D**), ATTO 590 is excited not only through FRET from dye **D** but also directly. Because  $\text{Cu}^{2+}$  quenches only the FRET component of ATTO 590 fluorescence, in the presence of saturating  $\text{Cu}^{2+}$  concentrations (5 equiv), considerable residual fluorescence of ATTO 590 is still present (~40%, Figure 7). Correspondingly,  $F_{534}/F_{624}$  is more strongly

dependent on the  $\text{Cu}^{2+}$  concentration (Figure 6) and the duplex DNA **1**/DNA **2** can be used as a ratiometric sensor for  $\text{Cu}^{2+}$ . Several sensors of this type have been reported for  $\text{Zn}^{2+}$ ,<sup>18</sup> however, to our knowledge, this is the first such sensor for  $\text{Cu}^{2+}$ .<sup>19</sup> The advantage of ratiometric sensors is that the ratio of fluorescence intensities is easier to quantify than absolute fluorescence intensities.

### Conclusions

We describe a modular approach for tuning of the emission wavelength of metal ion sensors. The principle of this approach has been demonstrated by sensing of  $\text{Cu}^{2+}$  ions. The intensity of sensor emission at 624 nm is strongly dependent on the  $\text{Cu}^{2+}$  concentration, with a 20 nM detection limit.

**Acknowledgment.** We thank the Deutsche Forschungsgemeinschaft (SFB 623) for financial support.

IC050362D

- (18) For example, commercially available ratiometric  $\text{Zn}^{2+}$  indicators are FuraZin-1 and IndoZin-1: <http://www.probes.com>.  
 (19) One ratiometric sensor for  $\text{Cu}^{2+}$  has been published after submission of this paper: Royzen, M.; Dai, Z.; Canary, J. W. *J. Am. Chem. Soc.* **2005**, *127*, 1612–1613.